HHS Public Access

Author manuscript

Polymer (Guildf). Author manuscript; available in PMC 2016 July 23.

Published in final edited form as:

Polymer (Guildf). 2015 July 23; 70: 8–18. doi:10.1016/j.polymer.2015.06.002.

Modification of linear prepolymers to tailor heterogeneous network formation through photo-initiated Polymerization-Induced Phase Separation

Caroline R. Szczepanski[a] and **Jeffrey W. Stansbury**[a,b]

[a]Department of Chemical and Biological Engineering, University of Colorado, Boulder, CO 80309, USA.

[b]Department of Craniofacial Biology, School of Dental Medicine, University of Colorado, Aurora, CO 80045, USA.

Abstract

Polymerization-induced phase separation (PIPS) was studied in ambient photopolymerizations of triethylene glycol dimethacrylate (TEGDMA) modified by poly(methyl methacrylate) (PMMA). The molecular weight of PMMA and the rate of network formation (through incident UV-irradiation) were varied to influence both the promotion of phase separation through increases in overall free energy, as well as the extent to which phase development occurs during polymerization through diffusion prior to network gelation. The overall free energy of the polymerizing system increases with PMMA molecular weight, such that PIPS is promoted thermodynamically at low loading levels (5 wt%) of a higher molecular weight PMMA (120 kDa), while a higher loading level (20 wt%) is needed to induce PIPS with lower PMMA molecular weight (11 kDa), and phase separation was not promoted at any loading level tested of the lowest molecular weight PMMA (1 kDa). Due to these differences in overall free energy, systems modified by PMMA (11 kDa) underwent phase separation via Nucleation and Growth, and systems modified by PMMA (120 kDa), followed the Spinodal Decomposition mechanism. Despite differences in phase structure, all materials form a continuous phase rich in TEGDMA homopolymer. At high irradiation intensity (I_o=20mW/cm^2), the rate of network formation prohibited significant phase separation, even when thermodynamically preferred. A staged curing approach, which utilizes low intensity irradiation (I_o=300μW/cm^2) for the first ~50% of reaction to allow phase separation via diffusion, followed by a high intensity flood-cure to achieve a high degree of conversion, was employed to form phase-separated networks with reduced polymerization stress yet equivalent final conversion and modulus.

Corresponding Author: Jeffrey W. Stansbury, Craniofacial Biology, Mail Stop 8120, 13065 E. 17th Avenue, Aurora, CO, 80045, jeffrey.stansbury@ucdenver.edu, (Ph): 001-303-724-1044, (Fax): 001-303-724-1945.

1. Introduction

The formation and design of heterogeneous polymer networks is a growing topic in materials science with applications in biomaterials, optical displays, membranes, adhesives, and composites[1–9]. For these uses, the ability to design a network with local property differentials, while maintaining bulk performance is highly desirable. Towards this design, two different approaches have been used most widely: the blending of two different polymers, or the formation of block copolymers[9–11]. When blending partially miscible prepolymers, heterogeneous morphology is controlled by the apparatus used for mixing, the rate or time used thereof, as well as the relative viscosities of each component[10, 12, 13]. Blending requires a large physical input to effectively distribute the components, and often needs to be performed at elevated temperatures[10, 12]. With the block copolymer approach precise initial preparation of monomers is necessary, as well as exact processing conditions (temperature, composition) to achieve the desired phase structure[11]. The ability to develop heterogeneous networks without these processing and synthetic constraints is desirable for many *in-situ* applications.

An alternate method to achieve network heterogeneity is through well-controlled polymerization-induced phase separation (PIPS). In this approach, a phase-separated network is formed from an initially homogenous, multi-component monomer formulation. The reaction of monomer to form polymer can lead to limited miscibility and if diffusion is possible, phase separation will occur to minimize the overall free energy. Since the phase separation occurs coincidentally with network formation, the extent to which immiscible phases diffuse from one another depends on the rate of polymerization, the onset of gelation and the degree of cross-linking at any given point during the reaction as well as any attractive or repulsive interactions between components in the formulation[14]. The dynamic interplay between the kinetics of network formation and thermodynamics of the polymerizing system is crucial to understanding and controlling the PIPS process[15]. PIPS has already shown promise for numerous applications including the development of polymer-dispersed liquid crystals[1–3, 5, 6, 8], poly-electrolyte membranes[7] as well as thermosets and composites[4].

Since PIPS depends heavily on the relationship between rate of network formation and the overall free energy of the system, being able to easily control either of these effects will allow for precise design of the final phase structure. Utilizing a photoinitiator to initiate the polymerization is an elegant approach to modulate the network kinetics and thus the rate of network formation. The relationship between polymerization kinetics and the photoinitiator loading, incident irradiation intensity and wavelength has been well studied and characterized[16]. Additionally, the use of light as the initiating mechanism allows for spatial and temporal control over the polymerization, which is advantageous for *in situ* applications.

Little work has been done to explore the control found when utilizing photoinitiation with PIPS. Previous investigations suggest that with increasing irradiation intensity and rate of polymerization, the characteristic length scale of morphology increases[17], and that the mechanism of phase separation will transition from Nucleation and Growth at low

polymerization rates to Spinodal Decomposition at higher rates[18]. Studies have also explored the effects of material thickness and temperature[19, 20], and the use of photo-PIPS has been explored to control morphology of polymer-dispersed liquid crystals[2, 3, 8]. However in the examples listed, if a multi-functional monomer is used it is at a very low volume fraction and the resulting network is loosely cross-linked and weak. Additionally, temperature is often utilized as a significant control parameter to vary phase structure. Limited work has explored the design of heterogeneous polymers with photo-PIPS in highly cross-linked networks formed under ambient conditions. For many applications, the elevated modulus and glass transition temperature of a network associated with dense cross-linking is highly favorable. However, the early onset of network gelation typical of densely cross-linked networks restricts diffusion of immiscible phases, which is a significant limitation to PIPS[21]. Therefore, it is crucial to understand what aspects of the polymerization can be addressed to promote PIPS during ambient photopolymerizations.

Our previous studies have demonstrated success in using photo-PIPS to develop heterogeneous morphology with a dimethacrylate homopolymer matrix modified by linear, non-reactive prepolymers[22, 23]. In the work presented here, we explore the use of prepolymer molecular weight as an approach to vary heterogeneous morphology formed through photo-PIPS. We demonstrate that by tailoring the prepolymer molecular weight while directly controlling the rate of network formation via photoirradiation, varying network morphologies can be formed. Previous work into the impact of prepolymer or additive size in heterogeneous networks formed via PIPS has focused on thermally cured epoxy-based resins[24]. Here, we show that using both prepolymer molecular weight and the rate of network formation we can define the limits where PIPS is restricted from physical and energetic limitations in an ambient-cured photopolymerization.

2. Experimental

2.1 Materials

Triethylene glycol dimethacrylate (TEGDMA, Esstech) was utilized as the bulk homopolymer matrix in this study. The matrix was modified by the addition of three different non-reactive, linear prepolymers. The prepolymers have the same repeat unit ((poly-methyl methacrylate); PMMA) but differ by an order of magnitude in molecular weight (discussed below). The photoinitiator in all studies was 2,2-dimethoxy-2-phenylacetophenone (DMPA), which absorbs in the UV-region. The loading of photoinitiator was kept at 0.5 wt% relative to the monomer/prepolymer mass. The irradiation source in all photopolymerizations was 365 (±10) nm.

2.1.1 Prepolymer Synthesis—Three different prepolymers of varying molecular weight, based on a methyl methacrylate repeat unit were developed to modify the homopolymer matrix. The highest molecular weight prepolymer utilized was commercially obtained (Aldrich; reported to have a weight average molecular weight (M_W) of 120 kDa and a polydispersity index (PDI) of 2.0). The remaining two prepolymers were prepared by a bulk thermal polymerization of methyl methacrylate in toluene, conducted at 65 °C for 3 h after which the temperature was elevated to 80 °C until reaching 95% conversion. The thermal initiator used was azobisisobutyronitrile (AIBN) at a loading level of 0.5 wt% relative to the

initial monomer mass. Conversion was monitored through the change in methacrylate peak area in the mid-IR (1635 cm^{-1}) with the carbonyl absorption used as an internal reference (1720 cm^{-1}). To modulate the resulting molecular weight, a chain transfer agent (dodecanethiol) was included in the reaction medium. The molar ratio of chain transfer agent to monomer was calculated based on the desired final molecular weight utilizing the Mayo Equation[25]. The final product was isolated by precipitation in hexanes. The molecular weight (determined by gel permeation chromatography (Viscotek triple detector) with tetrahydrofuran as eluent), glass transition temperature (T_g; determined by dynamic mechanical analysis (Perkin Elmer 8000) using 10 mg of the powdered prepolymer in thin aluminum pockets subjected to deflection of 50 μm at 1 Hz in air with heating at 2 °C/min), and refractive index (n_D^{22}, based on extrapolation from increasing concentrations of prepolymer in TEGDMA with a refractometer (Atago T2)) of the three different prepolymers are listed in Table 1.

2.2 Methods

2.2.1 Dynamic Mechanical Analysis—A dynamic mechanical analyzer (DMA, TA Q800) was used to characterize the thermal properties of networks post-cure. Samples had approximate dimensions (*length* × *width* × *thickness*) of 8 × 5 × 1 mm and were analyzed using a temperature sweep under 0.01% strain. After allowing the sample to equilibrate at −50 °C for 20 min, the samples were brought to a temperature of 200 °C at a rate of 3 °C/min, held isothermally at 200 °C for 20 min, and then cooled back to −50 °C at a rate of 3 °C/min. All samples were photopolymerized and then thermally post-cured at 180 °C to a conversion greater than 90% before DMA analysis so that no additional cure occurred as a result of the thermal scan. In select materials, conversion was monitored before and after the thermal scan in the DMA to further ensure no significant curing during the analysis. It was found that degree of methacrylate conversion might increase by 1–2% during the DMA scan, if at all. Since there already exists an error of ± 0.5 % in the final conversion measurements, any additional cure is minimal and should not affect the DMA data significantly. Results presented here are from the initial scan (increase) in temperature.

2.2.2 Optical Density during Polymerization—To measure optical properties during polymerization a UV/Vis portable spectrometer (Ocean Optics, USB2000) was used. A disc-shaped sample (thickness = 240 μm, diameter = 20 mm) was secured so that a near-IR source, visible light source, and UV curing light source could transmit simultaneously through the material. A Fourier transform infrared spectrometer (FTIR) with near-IR fiber optic cables (Thermo scientific, Nicolet 6700) was used as the near-IR source to simultaneously monitor methacrylate conversion. The degree of conversion was measured by monitoring the dynamic change in methacrylate peak area (=CH_2, first overtone at 6165cm^{-1}). To follow the changes in optical density of the polymerizing sample, the UV/Vis spectrometer was employed. A visible light source that emits broadband 400–800 nm wavelength light as a photo probe independent of the photoinitiator was used with the intensity of the 600 nm wavelength transmitted through the sample monitored in real time. The photoinitiator in this study (DMPA) does not absorb above 380 nm[26], so the visible light source did not alter the photopolymerization kinetics.

2.2.3 Viscosity—Monomer/prepolymer solution viscosities were measured using a parallel plate rheometer (TA Ares). To accomplish this, a steady rate sweep test (strain controlled) was done under ambient conditions. Sample dimensions were 0.200 mm thickness and 20 mm diameter. The initial rate was 0.1 and the final rate was 1000 (s^{-1}).

2.2.4 Tensometer—Real-time polymerization stress was measured under ambient photopolymerization conditions using a cantilever beam tensometer (Volpe Research Center, American Dental Association Health Foundation, Gaithersburg, MD). The tensometer was coupled with a Fourier transform infrared spectrometer (FTIR) with near-IR fiber optic cables (Thermo Scientific, Nicolet 6700) so methacrylate conversion could be observed simultaneously using the same conditions as described in the optical density experiments. This set-up was used to collect all kinetic data presented throughout this manuscript. All samples were disc shaped with 6 mm diameter and 1 mm thickness. The details of this instrument and its operation are described in greater detail in other publications[27].

2.2.5 Three-point Bending—Bar-shaped specimens of approximate dimension (*length* × *width* × *thickness*) 20 × 2 × 2 mm formed via ambient photopolymerization were tested in a universal testing machine (Mini Bionix 858, MTS). The machine was equipped with a 5 kN load cell for flexural strength and elastic modulus (n=3). All samples were tested with a crosshead speed of 1mm/min and a span of 15 mm between supporting rollers. The flexural modulus was calculated by extracting data from the initial linear portion of the load vs. displacement curve, and applying the formula:

$$\mathrm{E}=\frac{\mathrm{CL}^3}{4\mathrm{bh}^3\mathrm{d}} \times 10^{-3}$$

Where:

C=load at fracture (N)

d=displacement (mm)

L= distance between the supports (mm)

b= width of specimen (mm)

h= height of specimen (mm).

2.2.6 AFM Imaging—Heterogeneous networks were imaged using atomic force microscopy (AFM) in phase contrast imaging mode using an Easy Scan 2 (Nanosurf) AFM. Imaging was done under tapping mode using conical tapping mode AFM probes (Aspire CT-170), which have a spring constant of 50 N/m. Samples were prepared via ambient photopolymerization at various irradiance levels between glass slides (sample thickness ~ 1 mm).

3. Results & Discussion

The promotion of phase separation during polymerization is dictated by changes in overall free energy. In a multi-component polymerizing resin, the overall free energy is calculated through the Gibbs free energy of mixing:

$$\Delta G^{mix} = \Delta H^{mix} - T\Delta S^{mix}$$

When $\Delta G^{mix} > 0$, phase separation will occur, if possible, to achieve a lower overall free energy. In the phase-separating polymerizations studied here, changes in ΔG^{mix} are anticipated with changes in linear prepolymer chain length, as the entropy of mixing ΔS^{mix} will vary with this modification.

The entropy of mixing, ΔS^{mix}, depends directly on the degrees of freedom and number of conformations available for the different molecules in the polymerizing system. There are two main factors that contribute to the entropic term during PIPS, the first being the initial number of components in the system. To achieve an equivalent mass fraction loading level of prepolymer at different molecular weights, the number of prepolymer molecules introduced into the TEGDMA resin will have the following relationship:

$$n^{PMMA-120K} < n^{PMMA-11K} < n^{PMMA-1K}$$

The value for the entropy of mixing of each TEGDMA/PMMA formulation will follow this trend, as an increased number of molecules in the resin will increase the degrees of freedom. Thus, at any given loading level, in the monomeric state:

$$\Delta S^{mix}_{PMMA-120K} < \Delta S^{mix}_{PMMA-11K} < \Delta S^{mix}_{PMMA-1K}$$

Since the entropy of mixing is significantly lower with the higher molecular weight prepolymer, it will increase the overall free energy to a value higher than systems modified by PMMA-11K and PMMA-1K. Therefore, phase separation is expected to be more favorable in TEGDMA matrices modified by PMMA-120K. Another factor influencing the system entropy is the extent of conversion. As the polymerization proceeds and TEGDMA monomer molecules become part of the cross-linked network (which approaches a single molecule with infinite molecular weight), the entropy of mixing will decrease, making phase separation more favorable throughout the entire reaction. The decrease in entropy with methacrylate conversion will occur in systems modified by all three different prepolymers.

It should be noted that changes in entropy are not the only factors influencing overall free energy during PIPS. During polymerization, the chemical potential of the mixture, characterized by the Flory-Huggins interaction parameter will also change[28, 29]. Since this work focuses on TEGDMA matrices modified by PMMA of varying molecular weights, there should not be significant differences in interaction parameter between monomer and prepolymer as the prepolymer repeat unit is constant in all resins. However, as the molecular weight changes, the conformation of the prepolymer chains in the matrix change as well. At

higher molecular weights, the chain end concentration will decrease, which will impact how PMMA interacts both intra- and inter-molecularly with other PMMA chains and TEGDMA. These interactions can contribute to the overall free energy of the polymerizing material. We anticipate that the PMMA conformation does not vary significantly, as all TEGDMA/PMMA monomer solutions tested here behave as Newtonian fluids. If PMMA intermolecular interactions were significant there would be differences in solution viscosity as a function of shear rate, which were not observed in the materials tested here. Beyond this result, the changes in prepolymer conformation will not be a focus of this study.

Another factor influencing the chemical potential of the mixture is the presence of dodecanethiol, used to tailor PMMA molecular weight, on the PMMA chain ends. This effect is expected to be more significant on the lower molecular weight PMMA prepolymers, as more chain transfer agent was needed during prepolymer synthesis. However, since the formulations modified with PMMA-1K behave thermodynamically as expected based on the anticipated entropic changes due to number of PMMA prepolymer molecules (discussed next), this effect does not appear to be significant. To probe how the anticipated changes in entropy and free energy with PMMA molecular weight and number of molecules influence PIPS, dynamic mechanical analysis (DMA) was utilized to probe multi-phase structure post-polymerization, in TEGDMA matrices modified by the three different PMMA prepolymers.

3.1 Dynamic Mechanical Analysis

DMA was utilized after polymerization to evaluate thermal properties of the formed networks and to probe whether phase-separated domains formed. All materials analyzed via DMA were cured for 10 min at I_o=5 mW/cm^2. In these experiments all networks were also thermally post-cured after the ambient photopolymerization, at 180 °C for approximately 1 h to achieve a final conversion greater than 90% so that no additional cure occurs during the thermal scan (limiting conversion via ambient photopolymerization ranges from 70–85% methacrylate conversion depending on the formulation).

Tan delta profiles for materials modified by the intermediate molecular weight prepolymer, PMMA-11K are shown in Figure 1. The control matrix, poly(TEGDMA) displays one broad transition in the tan delta profile centered about 161 °C, indicating single-phase structure with a degree of structural heterogeneity, typical of dimethacrylate networks. When PMMA is added to the matrix at 20 wt% loading, secondary peak formation is observed at 125 °C, corresponding to the formation of a secondary phase rich in a combination of poly(TEGDMA) and PMMA-11K since the T_g has shifted to a value between that of poly(TEGDMA) and PMMA-11K (Table 1)[30]. A shoulder is still observed at ~161 °C indicating that a phase nearly exclusively comprised of poly(TEGDMA) remains. At lower loading levels (5 – 10 wt%), a single T_g is observed that has shifted to slightly lower temperatures than the poly(TEGDMA) control. This indicates that the system has not undergone phase separation, but instead the prepolymer remains uniformly dispersed throughout the matrix. The tan delta peak is also broadened at lower loading levels, indicating a slightly larger degree of heterogeneity compared to poly(TEGDMA) caused by the addition of prepolymer.

Tan delta profiles for TEGDMA matrices modified with PMMA-120K and PMMA-1K are included in the Supplemental Information. Two peaks are observed at all loading levels of PMMA-120K greater than 5 wt%, indicating phase separated structure (Supplemental Figure 1). With this prepolymer, even small additions can significantly increase the overall free energy to promote phase separation. In the matrices modified by PMMA-1K, no visible secondary peak formation is observed at any loading level up to 20 wt% (Supplemental Figure 2). However, there again is broadening of the tan delta peak with increasing prepolymer loading, and a slight shoulder in the 10 and 20 wt% modified samples. These shoulders are likely artifacts of forming a slightly more heterogeneous network than the poly(TEGDMA) control, and not a result of distinct phase structure formation. Additional characterization discussed throughout this study will demonstrate that the lack of secondary peak formation indicates that these networks do not undergo distinct PIPS and instead form broadly heterogeneous networks.

In the materials that display two transitions in the tan delta profile, the shift in T_g observed after polymerization can be used to estimate the composition of each phase formed. Since in all phase-separated materials studied here, one transition falls very close to that observed in bulk poly(TEGDMA), and the other falls between the T_g of poly(TEGDMA) and the T_g of the modifying PMMA, which varies based on the prepolymer molecular weight (Table 1), the two phases formed will be rich in TEGDMA and rich in TEGDMA/PMMA, respectively. The phase compositions in TEGDMA polymerizations modified by 20 wt% PMMA-11K and PMMA-120K were estimated by applying a modified version of the Fox Equation, displayed below[30], as both materials displayed distinct secondary peak formation.

$$TEGDMA\ Fraction = 1 - \left(\frac{\left(T_g^{poly(TEGDMA)} - T_g^{NewPhase} \right)}{\left(T_g^{poly(TEGDMA)} - T_g^{PMMA} \right)} \right)$$

It should be noted that the experimentally observed poly(TEGDMA) T_g, which has an associated error of ± 4.0 °C, is utilized in the Fox Equation. Therefore, it is possible to calculate a phase composition greater than 1, since the error in the Fox Equation associated with the variation in poly(TEGDMA) T_g is ± 0.07. All T_g's associated with a TEGDMA-rich domain fell within error of that observed for the pure poly(TEGDMA) homopolymer (Table 2).

The TEGDMA-rich phase is expected to be a continuous domain in both materials probed, as TEGDMA is the major component in the initial resin. The TEGDMA/PMMA-rich phase varies in composition depending on PMMA molecular weight. The highest molecular weight prepolymer, PMMA-120K forms a secondary phase that is much more concentrated in PMMA. This finding, along with the observation that PMMA-120K effectively induces phase separation at lower loading levels, indicates that the thermodynamic instability during polymerization varies based on prepolymer chain length. Additionally, the differences in phase composition indicate that there should be an observed difference in volume fraction of the TEGDMA/PMMA-rich phase, which will be validated later in this study.

Thus far, these studies have identified how PMMA chain length influences the overall free energy of a polymerizing resin, affecting whether PIPS is promoted. However, analysis of the resulting phase compositions indicates that even in two materials where the overall free energy is sufficiently high and PIPS is promoted, the resulting phase structure and composition varies. To begin to probe the differentials in the phase separation process amongst systems with sufficiently high free energy, light transmission behavior was observed during polymerization.

3.2 Turbidity measurements during polymerization

The transmission of visible light (λ = 600nm) was monitored during ambient photopolymerizations to characterize phase separation. All TEGDMA/PMMA samples begin as optically clear monomer formulations with essentially equivalent initial light transmission values. The decrease in prepolymer refractive index (Table 1) with increasing PMMA size was unexpected since density and presumably refractive index typically increase with polymer molecular weight[31]. Figure 2 displays visible light transmission as a function of conversion through TEGDMA-modified networks during polymerization (I_o=5 mW/cm^2).

During the photocure of TEGDMA/20 wt% PMMA-1K, there is little change in light transmission, indicating no significant difference in refractive index across the material during polymerization, which is an additional indication that phase separation does not occur in polymerizations modified by PMMA-1K. This behavior is identical to the visible light transmission during a poly(TEGDMA) bulk polymerization. There are slight deviations from I/I_o=1 during both reactions, which is likely due to microgel formation and small heterogeneities associated with a dimethacrylate polymerization, as well as noise in the measurement process.

When TEGDMA is modified with 10 wt% PMMA-120K or 20 wt% PMMA-11K, both materials which display multiple peaks in their tan delta profiles (Figure 1, Supplemental Figure 1), there is an observed decrease in visible light transmission at very early stages of the polymerization. This occurs between 1–7 % methacrylate conversion depending on the specific formulation, and is attributed to the onset of phase separation with the formation of partially immiscible phases; one rich in TEGDMA and one rich in TEGDMA/PMMA with differing refractive indices. The phase enriched with PMMA will initially have a higher refractive because of the relatively high prepolymer content compared to the TEGDMA-rich phases.

The visible light transmission in the TEGDMA/10wt% PMMA-120K sample decreases until approximately 20% methacrylate conversion. During this period, the refractive index difference between compositionally different phases increases, as one phase polymerizes more rapidly and reaches a higher local extent of conversion, as conversion of monomer into polymer will increase refractive index in a linear manner[32]. Specifically, the TEGDMA-rich phase, which has a lower local viscosity and higher local double bond concentration will initially polymerize more rapidly. The PMMA-rich phase, with a higher viscosity will develop at a slower rate[22]. For comparison, the refractive index of TEGDMA begins at about 1.460 and approaches a limiting value of ~1.53 during ambient condition

photopolymerization[33], which is higher than that of the pure prepolymers (Table 1). An additional effect that may be enhancing the decrease in light transmission is further changes in the composition of each phase through continued diffusion of monomer or prepolymer, although this effect will be minimized by gelation, which is delayed significantly to 10–20% methacrylate conversion in the bulk[21]. This delayed gelation is again a result of the formation of two co-continuous domains, polymerizing at nonequivalent rates. After the light transmission minimum at about 20% methacrylate conversion, a recovery to ~95% of the initial visible light transmission is observed in the TEGDMA/10wt% PMMA-120K polymerization. This occurs as the TEGDMA/PMMA-enriched phase, which polymerizes more slowly, approaches a level of network development closer to that of the TEGDMA-enriched domains, thus minimizing the refractive index differential between the two phases caused by local variations in conversion[32, 33]. At the end of polymerization when both phases have reached limiting conversion, there will be compositional differences between the domains, as demonstrated through shifts in T_g (Table 2), and this causes a modest refractive index mismatch, and a slight decrease in light transmission compared to the control resin.

In the TEGDMA/20wt% PMMA-11K sample, reduction in visible light transmission begins slightly later with respect to conversion compared to TEGDMA/10 wt% PMMA-120K. Additionally, the visible light reduction continues throughout much more of the reaction, and there is a less significant recovery period at the end of the ambient cure. This indicates significant differences in the phase separation with variation of PMMA chain length. To illustrate these differences, a variation of a phase diagram was produced (Figure 3) as a function of conversion for polymerizations modified by PMMA-120K at various loadings, and PMMA-11K at 20 wt% loading. Since PIPS is not detected at any loading level when PMMA-1K is the modifier, there is no phase boundary displayed for these polymerizations. The first phase boundary, the onset of PIPS as observed by decreases in visible light transmission, is indicated with filled circles (PMMA-120K) and open circles (PMMA-11K). PIPS is induced very early when PMMA-120K is the modifier and when the chain length is decreased PIPS is delayed and the phase boundary shifts to higher degrees of conversion. The conversion at which the minimum level of light transmission is observed is also plotted in the phase diagram (filled squares - PMMA-120K, open squares PMMA-11K). This was chosen, as it can be assumed that beyond this point no further significant changes in phase composition occur, as diffusion of both PMMA and free monomer are severely limited, so this boundary can be considered an end point for phase separation. Again, this boundary occurs at a much later stage of conversion with PMMA-11K compared to PMMA-120K.

Thus far, the changes in free energy due to modification of prepolymer molecular weight in a TEGDMA/PMMA polymerization have been explored. At lower loading levels of prepolymer, phase-separated networks are only observed in the TEGDMA/PMMA-120K networks as it is the only resin with entropy of mixing sufficiently low to promote phase separation. At higher prepolymer loadings (20 wt%) the combined effects of high prepolymer content and decreased TEGDMA concentration promotes PIPS in the formulations modified in both PMMA-11K and PMMA-120K, however the entropic contributions to the overall free energy in these two systems are non-equivalent as indicated in the phase diagram (Figure 3). The lowest molecular weight prepolymer, PMMA-1K does

not undergo phase separation at any of the loading levels tested here, as it has the highest entropy of mixing.

Beyond the changes in the overall free energy, an effect that must be considered in PIPS is that the kinetic and physical parameters are changing throughout the polymerization process. Increases in viscosity, formation of cross-links, gelation, and vitrification can significantly limit the extent to which PIPS can occur through diffusion during polymerization. For instance, two material systems undergoing PIPS that both have a sufficiently high free energy may achieve drastically different phase structures and compositions based on the rate of network formation. If the polymerization is rapid, the period allowed for PIPS via diffusion before the network gels (and presumably locks heterogeneous structure into place) will be limited and will restrict the domain size and composition that can form. In this scenario, the network may never achieve thermodynamic equilibrium as PIPS is suppressed very early during polymerization. If network formation is much slower, and the time available for diffusion of immiscible phases after the onset of phase separation is greater, a material can form well-developed, regular phase structure through diffusion prior to gelation.

Our previous work into PIPS in a TEGDMA-based matrix has shown that the resulting phase structure relies heavily on the average polymerization rate and the amount of time between the onset of phase separation and the onset of network gelation[21, 23]. Therefore, the remainder of this study will focus on how PMMA molecular weight influences the kinetic development and diffusion within phase-separated networks. To study this, a constant PMMA-loading level (20 wt%) was chosen for analysis throughout the remainder of the study.

3.3 Kinetics of Polymerization during PIPS

The polymerization rate behavior during the reaction is greatly affected by the viscosity of the initial monomer solutions in addition to the heterogeneous phase compositions that ensue. The viscosity of each TEGDMA/PMMA solution was measured in the monomeric state (Table 3). As is expected, the viscosity increases with the molecular weight of prepolymer, while all resins display Newtonian fluid behavior. The most significant increase occurs between the PMMA-11K and 120K, as the viscosity increases by a factor of ~40 as opposed to 1.6 and 5-fold increases, respectively.

The differences in viscosity of the initial formulations influence the polymerization kinetic behavior. When the irradiation intensity is sufficiently high (I_o=20 mW/cm^2), no difference is observed in polymerization rate behavior across the three different modifying prepolymers (Supplemental Figure 3). All three have nearly instantaneous increase in kinetic rate that is more rapid than in the control poly(TEGDMA) polymerization. The increased viscosity of PMMA-modified monomer solutions (Table 3) favors autoacceleration and diffusion-limited termination early on in the reaction, leading to a relatively higher overall rate of polymerization compared to bulk poly(TEGDMA). All materials achieve a similar final methacrylate conversion of 80%.

The overall polymerization rates decrease, as expected, when the irradiation intensity is decreased to I_o=300 μW/cm^2 (Figure 4). It should be noted, that the observed decrease in polymerization rate of the control matrix poly(TEGDMA), was not as significant as expected. A half order dependence of incident irradiation intensity (I_o) on the resulting polymerization rate (R_p) has been characterized for bulk, cross-linking free radical polymerizations[34]. With the intensities tested here, which vary by a factor of 66, an 8-fold decrease is expected in the polymerization rate of poly(TEGDMA). With closer evaluation of the poly(TEGDMA) kinetics presented here, it is found that the scaling factor (which, as stated, is expected to be ~0.5) between I_o and R_p varies during the polymerization. Up to ~40% conversion, the scaling factor is roughly 0.3, but then steadily increases with further methacrylate conversion, reaching a value of 0.4 at 80% conversion. Both the variation in the scaling factor with conversion, as well as the dependence on initiation rate that scales less than the traditional value of 0.5 at early stages of the reaction, have been characterized during the polymerization of multi-functional methacrylates[35–37]. The deviation from the half order scaling law at early stages of the reaction is due to chain-length dependent termination kinetics[35], while the portion of the reaction where the scaling factor varies with conversion (encountered after 40% methacrylate conversion) indicates that the polymerization is transitioning to a regime where termination is controlled by reaction diffusion[36].

Most importantly, at the lower irradiation intensity (I_o=300 μW/cm^2), differences are observed in the bulk polymerization rate as a function of modifying prepolymer molecular weight. The TEGDMA/20 wt% PMMA-1K and TEGDMA/20 wt% PMMA-11K polymerizations have identical rate profiles with slightly lower rates of polymerization compared to the control, poly(TEGDMA). However, the TEGDMA/20 wt% PMMA-120K polymerization has an enhanced autoacceleration behavior, reaching a higher maximum rate of polymerization (R_p^{max}) at a later stage of the reaction and having a higher limiting methacrylate conversion compared to the other PMMA-modified systems. Since the viscosity of PMMA-modified systems is much higher, the limiting conversion decreases due to diffusion constraints, all three PMMA-modified matrices have limiting conversions less than that of poly(TEGDMA).

We suspect that the lower polymerization rate when the irradiation intensity is decreased allows for more distinct phase-separated structure to form compared to the polymerizations conducted at much higher irradiation intensities, since there is more time for diffusion of immiscible phases prior to the onset of viscous effects such as gelation that prohibit PIPS. Additionally, the observed differences in polymerization rate with PMMA molecular weight during the slow kinetic regime (Figure 4) indicate there are significant differentials in phase morphology (which will be addressed shortly), as well as phase composition (Table 2). The remainder of this study will focus on demonstrating how both the kinetic variations as well as changes in overall free energy must be addressed and understood to design and engineer phase-separated networks.

3.4 Stress Reduction through PIPS

To demonstrate the influence of both polymerization kinetics and overall free energy on designing networks via PIPS, polymerization stress development was evaluated in TEGDMA/PMMA matrices while varying the PMMA molecular weight and the rate of network formation (through incident UV-irradiation intensity). Formation of phase-separated networks has been explored as an approach to reduce polymerization stress[4, 38, 39]. In a TEGDMA-based polymerization, we have found that networks formed via photo-PIPS often display a reduction in polymerization stress while maintaining an equivalent modulus. For effective stress reduction, ample amount of pre-gel network development between the onset of phase separation and the onset of network gelation is needed to allow for development of two co-continuous phases[4, 21].

In the studies here, the variation of prepolymer molecular weight significantly alters the ability of the prepolymer to diffuse throughout the reaction medium. Additionally, since the prepolymer molecular weight also impacts the solution viscosity (Table 3), the modification of PMMA molecular weight also has an effect on monomer diffusion, which is equally if not more important and more likely than prepolymer diffusion. These changes in diffusivity throughout the reaction medium during polymerization may impact the extent to which phase structure develops in the TEGDMA/PMMA networks. By varying the rate of network formation, the amount of time between phase separation and gelation can be shortened or extended based on the curing intensity employed. In the TEGDMA/PMMA polymerizations studied here, suppression of phase separation is encountered when polymerizations are conducted at high incident irradiation intensity (I_o=20 mW/cm^2). At this rate of network formation, the control homopolymer network, poly(TEGDMA), experiences ~2.0 MPa stress at the end of ambient photopolymerization. When the TEGDMA matrix is modified at a loading level of 20 wt% by the PMMA prepolymers the final polymerization stress is 1.55 MPa (Supplemental Figure 4), and this result does not vary with the prepolymer molecular weight. The reduction in polymerization stress with PMMA modification scales with the loading level of prepolymer, indicating it is an artifact of the decrease in double bond concentration, which for a fixed level of conversion will produce less shrinkage strain. Since diffusion is limited at this high rate of polymerization, distinct phase structures that provide interfaces that compensate for polymerization stress reduction through internal volume rearrangement do not form. This result is expected, as kinetic analysis of PMMA-modified resins at this irradiation regime (Supplemental Figure 3) displayed no differences as a function of PMMA molecular weight.

If the rate of network formation is slowed down, thus allowing for more diffusion of partially miscible phases, the stress reduction should go beyond the effect of decreased double bond concentration based on the addition of prepolymer. To probe this, the polymerization stress development was evaluated during a ‘staged curing’ ambient photopolymerization (Figure 5). The initial irradiation intensity was set to I_o=300 μW/cm^2 until 50% methacrylate conversion was achieved. This was monitored using FTIR spectroscopy simultaneously with the tensometer used to measure polymerization stress. After this point, the irradiation intensity was increased to I_o=20 mW/cm^2 for the remainder of the polymerization, to achieve a sufficiently high final degree of conversion. This

benchmark (50% methacrylate conversion) was chosen as the point to switch between low and high irradiation intensity since it is well beyond the gel point, and thus heterogeneous structure can reasonably be assumed to be locked in place by this stage. The initial low intensity cure was chosen, as it has already been demonstrated to lead to differentials in kinetic behavior based on the modifying PMMA and likely variations in phase separation behavior (Figure 4).

As seen in Figure 5, using this staged curing approach there is an observed difference between polymerization stress reduction based on the molecular weight of the modifying prepolymer. Just as in the completely high irradiation polymerization (Supplemental Figure 4), the poly(TEGDMA) control has a final polymerization stress of 2.0 MPa. The TEGDMA/ 20 wt% PMMA-1K develops ~1.6 MPa of stress, a value that scales with the loading level of prepolymer. This further supports that as the molecular weight of the prepolymer becomes sufficiently low, it does not impose any thermodynamic instability during polymerization and thus behaves like inert filler in the matrix. The networks modified with PMMA-11K and PMMA-120K have ~35–45% reduction in polymerization stress compared to the poly(TEGDMA) matrix. In these networks, the combination of higher overall free energy promoting PIPS and sufficient time prior to network gelation allow for the formation of phase-separated structure. This structure formation allows for more efficient compensation of volumetric shrinkage and polymerization stress, which has been characterized in detail[21].

A benefit of utilizing this staged curing approach is that we can develop phase-separated networks utilizing the low intensity initial cure, but by employing the late stage flood cure the materials can achieve certain critical bulk properties (such as degree of conversion and modulus) at the end of the polymerization. To confirm this, the bulk elastic modulus of poly(TEGDMA) and TEGDMA/PMMA matrices cured under varying light intensities, was evaluated post-ambient photopolymerization (Figure 6).

In some cases, there is a modest difference in final modulus between materials formed using a high intensity irradiation (I_o=20mW/cm^2) for the entire polymerization or employing the staged curing (20 wt% PMMA-11K, 20 wt% PMMA-120K). This is due to the differences in reaction exotherm from the different curing methods. In all materials, when the networks are formed under low irradiation intensity, (I_o=300 μW/cm^2) the resulting bulk modulus is decreased significantly, mostly because these materials do not achieve an equivalent final degree of conversion. Again, this shows that by understanding the limitations to diffusion of incompatible or partially miscible phases, processing procedures can be designed that allow for distinct phase-separated network formation via PIPS without compromise in desired final properties such as bulk modulus.

The last point to be addressed in this study is the difference observed in the phase separation process in the 11K and 120K modified networks. When TEGDMA is modified by 20wt% of either of these PMMA prepolymers, the free energy is sufficiently high to promote PIPS. However, many differentials in the phase behavior and bulk network development are observed between these polymerizations. Under low irradiance conditions, the initial rates of network formation vary significantly (Figure 4). Since TEGDMA / 20 wt% PMMA-120K

has a higher viscosity, and an extended autoacceleration period, this serves as a first indication that a greater extent of phase development can occur prior to viscous effects prohibiting further phase evolution. Additionally, the visible light transmission behavior through the PMMA-11K modified networks is quite different from that of the PMMA-120K network (Figure 2). Lastly, the absolute degree of stress reduction at the completion of ambient photopolymerization varies between 35% for TEGDMA/20wt% PMMA-11K, and 45% for TEGDMA/20wt% PMMA-120K (Figure 5). This could result from differences in domain size or the mechanism of phase separation that is occurring during polymerization, as it has been cited that co-continuous structure is more effective at shrinkage reduction[4].

3.5 Phase structure imaging through atomic force microscopy (AFM)

To probe differences in resulting phase structure, AFM was utilized to image materials cured at different irradiation intensities post-polymerization. When poly(TEGDMA) homopolymer was analyzed, no distinct phase structure on the micron length scale was observed, as is expected with the control, which is compositionally homogeneous (Supplemental Figure 5). When TEGDMA/PMMA-1K materials were imaged post-cure, they appeared identical to the poly(TEGDMA) control (Supplemental Figure 6), which further supports our claim that with a sufficiently low prepolymer molecular weight, PIPS is not favored during the TEGDMA/PMMA photopolymerization.

When the modifying prepolymer molecular weight is increased to 11K, phase-separated structure is observed (Figure 7), as expected. If the network is formed rapidly (I_o=20 mW/cm^2), as in Figure 7A, there are very small spherical domains on the order of 100 nm in diameter, and the material remains transparent during polymerization. However, these spherical domains are dispersed within a continuous matrix. When the material is polymerized at a slower rate, as in 7B and 7C, much larger spherical domains are present throughout the entire matrix with diameters varying from 0.5–1 μm. In both kinetic regimes, phase structure characteristic of the Nucleation and Growth phase separation mechanism, results. It is not surprising that in the slower polymerization, the spherical domains increase in size, as the decrease in rate of network formation will allow for coalescence and growth prior to network gelation.

The composition of the two phases formed through PIPS in TEGDMA/20wt% PMMA-11K has been estimated (Table 2): one being TEGDMA-rich and one being TEGDMA/PMMA-rich. In the images presented below, we anticipate that the TEGDMA-rich domains are the continuous phase, as there is a much more significant volume fraction of TEGDMA monomer in the initial resin. Additionally, we expect that the TEGDMA-rich domains polymerize more rapidly, and therefore can form an interconnected, continuous domain readily. However, when this continuous network forms more slowly there is more time for diffusion and coalescence of the dispersed TEGDMA/PMMA rich domains, which accounts for the increase in domain size as the irradiation intensity decreases. This result also shows promising evidence that phase morphology can be manipulated with the rate of network formation. It is unlikely that a phase inversion could be achieved with further decrease of the polymerization rate, as the reaction in the TEGDMA-rich domains will still proceed more

rapidly compared to the TEGDMA/PMMA-rich domains, promoting the formation of a TEGDMA continuous phase.

With the highest prepolymer molecular weight modification (TEGDMA/20wt% PMMA-120K), phase morphology also varies with rate of network formation (Figure 8). When the network is formed rapidly, there is no observable distinct phase structure. Broad, structural heterogeneities are observed when the sample is scanned over an area of 20 μm or more. However these irregularities are not regular in size or shape (Figure 8A). When the sample is scanned over an area smaller than 20 μm, no heterogeneity is observed (Figure 8B). In this case, phase separation is limited by the rapid rate of network formation, and the broad structural heterogeneities observed in Figure 8A are a result of incomplete phase separation as there is insufficient time available for diffusion of immiscible phases. When the initial rate of network formation is slower, as permitted by employing staged curing, phase-separated structure is observed (Figure 8C–D). In the networks modified by PMMA-120K, the domains appear to be more co-continuous, indicative of the Spinodal Decomposition mechanism[4, 40]. In this polymerization a TEGDMA-rich and TEGDMA/ PMMA-rich phase also develops (Table 2). Again, the TEGDMA-rich domain is expected to develop more rapidly. It may grow in size, as free TEGDMA monomer will diffuse to these regions during initial stages of the reaction. After the onset of network gelation (at 10–20% bulk conversion as previously demonstrated in analogous TEGDMA/prepolymer compositions [23]), the phase morphology will not vary significantly, as diffusion is significantly limited.

The differences in resulting phase structure between materials modified with PMMA-11K and PMMA-120K are not unexpected based on the studies presented here. With PMMA-120K as a modifier, the entropy of the polymerizing system is lowest. This leads to the material system with the highest free energy tested, and could promote a highly unstable thermodynamic state during polymerization, resulting in the Spinodal Decomposition mechanism. In the system modified by PMMA-11K, the higher degree of entropy results in the system only becoming metastable during polymerization, forming a dispersed phase structure typical of Nucleation and Growth, as seen in Figure 7[40]. The much larger domain sizes that form in TEGDMA/ 20wt% PMMA-11K materials indicate that coalescence, and diffusion of incompatible phases is less hindered in this polymerization as the viscosity is lower (Table 3), and also reflects the difference in phase composition of the TEGDMA/PMMA-rich phase, calculated earlier (Table 2). Lastly, the polymerization stress is reduced less significantly in the TEGDMA / 20wt% PMMA-11K material, which supports the previously proposed claim that phase structure resulting from the Nucleation and Growth mechanism is less efficient at stress reduction[41]. This is supported by the co-continuous network structure and higher degree of stress reduction observed in the network modified by PMMA-120K.

4. Conclusions

Here we have demonstrated the ability to use prepolymer molecular weight to adjust the overall free energy of a TEGDMA polymerization modified by linear PMMA prepolymer, to either promote or suppress polymerization-induced phase separation (PIPS). When the

modifying prepolymer has a very low molecular weight (1,000 Da, PMMA-1K), phase separation is never favored during the polymerization, as indicated by tan delta behavior post-cure, up to loading levels of 20 wt% PMMA. At intermediate prepolymer molecular weights (11,000 Da, PMMA-11K), PIPS is observed at loading levels of 20 wt%, and when the prepolymer molecular weight is further increased to 120,000 Da, PIPS is observed at all loading levels tested. As the prepolymer molecular weight increases, the overall system entropy decreases, promoting PIPS since the overall free energy is much higher and closer to the instability threshold throughout the reaction.

Understanding the impact of prepolymer molecular weight on the overall free energy from these results, we explored how the network design could be more precise by controlling the rate of network formation through photoirradiation. When the rate of network formation is sufficiently high (I_o=20 mW/cm^2), PIPS is suppressed significantly. No enhanced stress reduction is observed in these polymerizations and no distinct phase structure is observed. When a staged curing approach is taken, where the sample is first initiated under low light intensities (I_o=300 μW/cm^2) until 50% methacrylate conversion, followed by high-intensity curing (I_o=20 mW/cm^2) for the remainder of the reaction, PIPS occurs in the systems modified by PMMA-11K and PMMA-120K. When modified by PMMA-11K, the resulting phase structure is dispersed with a TEGDMA continuous network and a TEGDMA/PMMA dispersed domain, indicative of the Nucleation and Growth mechanism and a 35% reduction in polymerization stress compared to poly(TEGDMA). The size of the resulting phase structure can be tailored with the irradiation intensity employed, as a lower intensity will allow for a greater extent of diffusion and the formation of larger dispersed domains. When PMMA-120K is the modifying prepolymer, the phase structure is co-continuous, indicative of the Spinodal Decomposition mechanism of phase separation, and the observed stress reduction is 45% with no significant decrease in bulk modulus.

This study demonstrates that the combined effects of preoplymer molecular weight and rate of network formation can be used to precisely design heterogeneous networks formed via PIPS. Even though a multi-functional monomer that forms a densely cross-linked network is used as the bulk material, differing phase structures and domain sizes can form. The formation of these differing heterogeneities depends on both the rate of network formation, or the kinetics of network formation, as well as the overall free energy of the polymerizing system.

Supplementary Material

Refer to Web version on PubMed Central for supplementary material.

Acknowledgements

The donation of monomer used in this study by Esstech, the microscope access from the University of Colorado Nanomaterials Characterization Facility, as well as funding support from NIH R01DE022348 are greatly appreciated.

References

1. Boots HMJ, Kloosterboer JG, Serbutoviez C, Touwslager FJ. Macromolecules. 1996; 29(24):7683–7689.
2. Serbutoviez C, Kloosterboer JG, Boots HMJ, Touwslager FJ. Macromolecules. 1996; 29(24):7690–7698.
3. Serbutoviez C, Kloosterboer JG, Boots HMJ, Paulissen F, Touwslager FJ. Liquid Crystals. 1997; 22(2):145–156.
4. Li W, Lee LJ. Polymer. 2000; 41(2):685–696.
5. Smith DM, Li CY, Bunning TJ. Journal of Polymer Science Part B-Polymer Physics. 2014; 52(3): 232–250.
6. Park S, Kim HK, Hong JW. Polymer Testing. 2010; 29(7):886–893.
7. Schulze MW, McIntosh LD, Hillmyer MA, Lodge TP. Nano Letters. 2014; 14(1):122–126. [PubMed: 24328570]
8. Kihara H, Miura T. Polymer. 2005; 46(23):10378–10382.
9. Clapper JD, Skeie JM, Mullins RF, Guymon CA. Polymer. 2007; 48(22):6554–6564.
10. Willemse RC, Ramaker EJJ, van Dam J, de Boer AP. Polymer. 1999; 40(24):6651–6659.
11. Lipic PM, Bates FS, Hillmyer MA. Journal of the American Chemical Society. 1998; 120(35): 8963–8970.
12. Willemse RC, Ramaker EJJ, Van Dam J, De Boer AP. Polymer Engineering and Science. 1999; 39(9):1717–1725.
13. Veenstra H, Van Dam J, de Boer AP. Polymer. 2000; 41(8):3037–3045.
14. Zheng X, Rafailovich MH, Sokolov J, Strzhemechny Y, Schwarz SA, Sauer BB, Rubinstein M. Physical Review Letters. 1997; 79(2):241–244.
15. Schroeder WF, Aranguren MI, Elicabe GE, Borrajo J. European Polymer Journal. 2013; 49(12): 3956–3965.
16. Berchtold KA, Hacioglu B, Lovell L, Nie J, Bowman CN. Macromolecules. 2001; 34(15):5103–5111.
17. Van-Pham, D-T. Phase separation kinetics and morphology induced by photopolymerization of 2-hydroxyehyl methacrylate (HEMA) in poly(ethyl acrylate)/HEMA mixtures. In: Tran-Cong-Miyata, Q., editor. Advances in Natural Sciences: Nanoscience and Nanotechnology. Vol. 4. 2013. p. 7
18. Kimura N, Kawazoe K, Nakanishi H, Norisuye T, Tran-Cong-Miyata Q. Soft Matter. 2013; 9(35): 8428–8437.
19. Qui TCM, Kinohira T, Van-Pham T, Hirose A, Norisuye T, Nakanishi H. Current Opinion in Solid State & Materials Science. 2011; 15(6):254–261.
20. Murata K, Sachin J, Etori H, Anazawa T. Polymer. 2002; 43(9):2845–2859.
21. Szczepanski CR, Stansbury JW. Stress reduction in phase-separated, cross-linked networks: Influence of phase structure and kinetics of reaction. Journal of Applied Polymer Science. 2014
22. Szczepanski CR, Pfeifer CS, Stansbury JW. Polymer. 2012; 53(21):4694–4701. [PubMed: 23109733]
23. Szczepanski CR, Stansbury JW. European Polymer Journal. 2015; 67(0):314–325. [PubMed: 25954051]
24. Liu Y, Zhong XH, Yu YF. Colloid and Polymer Science. 2010; 288(16–17):1561–1570.
25. Odian, G. Principles of Polymerization. Fourth ed. Hoboken: Wiley & Sons; 2004.
26. Green, WA. Industrial Photoinitiators - A Technical Guide. Boca Raton, FL: CRC Press -Taylor & Francis Group; 2010.
27. Lu H, Stansbury JW, Dickens SH, Eichmiller FC, Bowman CN. Journal of Materials Science-Materials in Medicine. 2004; 15(10):1097–1103. [PubMed: 15516870]
28. Flory PJ. Journal of Chemical Physics. 1941; 9(8):660–661.
29. Lipatov YS. Polymer Bulletin. 2007; 58(1):105–118.
30. Fox TG, Loshaek S. Journal of Polymer Science. 1955; 15(80):371–390.

31. Bowden MJ, Chandros Ea, Kaminow IP. Applied Optics. 1974; 13(1):112–117. [PubMed: 20125930]
32. Howard B, Wilson ND, Newman SM, Pfeifer CS, Stansbury JW. Acta Biomaterialia. 2010; 6(6): 2053–2059. [PubMed: 19913646]
33. Lehtinen J, Laurila T, Lassila LVJ, Vallittu PK, Raty J, Hernberg R. Dental Materials. 2008; 24(10):1324–1328. [PubMed: 18420264]
34. Decker C. Macromolecular Rapid Communications. 2002; 23(18):1067–1093.
35. Lovestead TM, Berchtold KA, Bowman CN. Macromolecules. 2005; 38(15):6374–6381.
36. Berchtold KA, Lovestead TM, Bowman CN. Macromolecules. 2002; 35(21):7968–7975.
37. Anseth KS, Kline LM, Walker TA, Anderson KJ, Bowman CN. Macromolecules. 1995; 28(7): 2491–2499.
38. Velazquez R, Sanchez F, Yanez R, Castano VM. Journal of Applied Polymer Science. 2000; 78(3): 586–591.
39. Cao X, Lee LJ. Journal of Applied Polymer Science. 2003; 90(6):1486–1496.
40. Nishi T, Wang TT, Kwei TK. Macromolecules. 1975; 8(2):227–234.
41. Li W, Lee LJ. Polymer. 2000; 41(2):697–710.

- Phase separation was studied in TEGDMA matrices modified by PMMA
- Three different PMMA chain lengths were explored: 1kDa, 11kDa, 120kDa
- Increased PMMA chain length decreased free energy and favored phase separation
- Rate of network formation was modulated to change the extent of phase separation
- TEGDMA/PMMA networks with significantly reduced stress were designed.

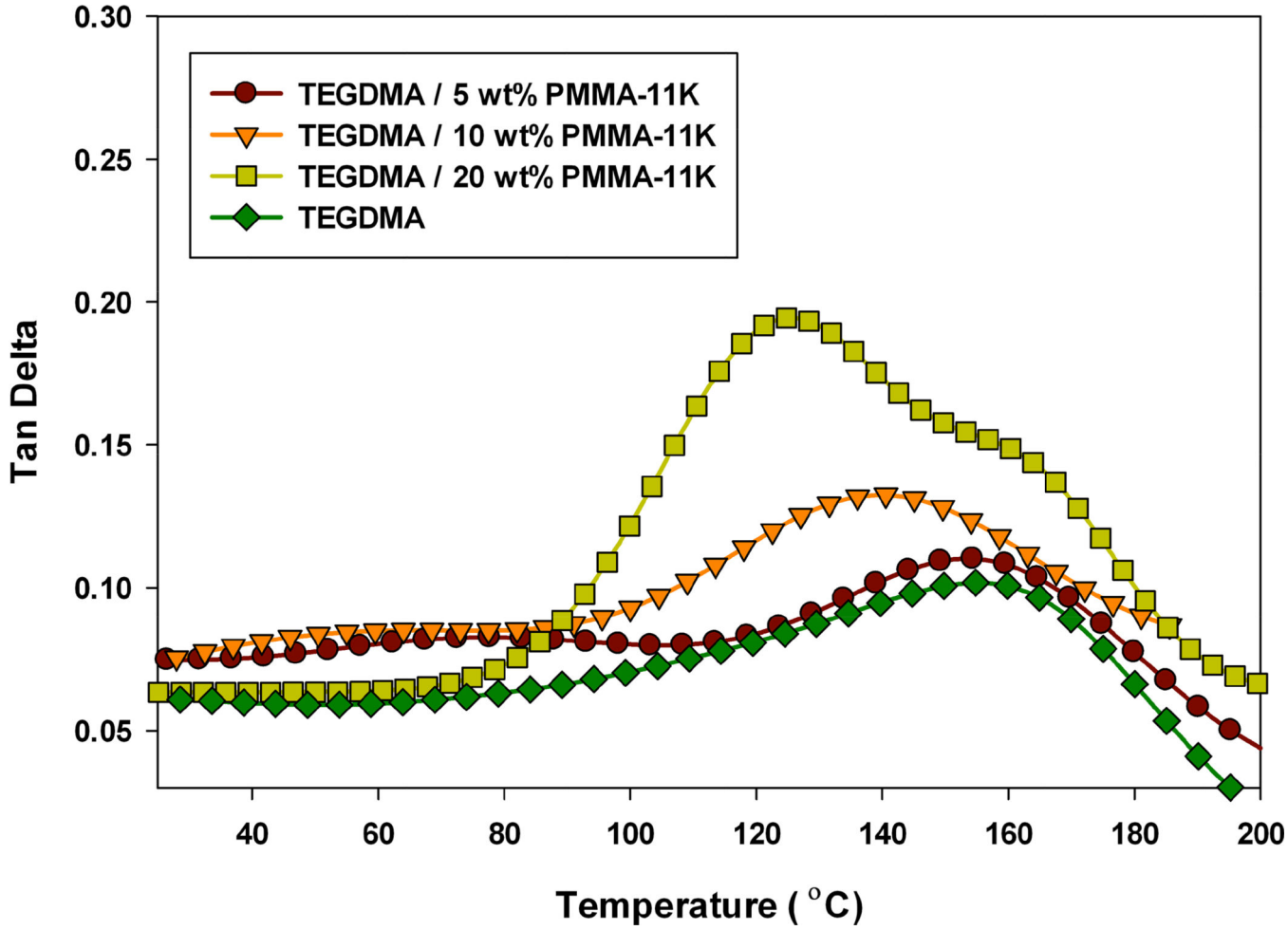

Figure 1.

Tan delta profile post-cure of poly(TEGDMA) networks modified by PMMA-11K. All networks were photopolymerized under ambient conditions (I_o=5 mW/cm^2) and post-thermally cured for 1 h at 180 °C to reach a final conversion >90%.

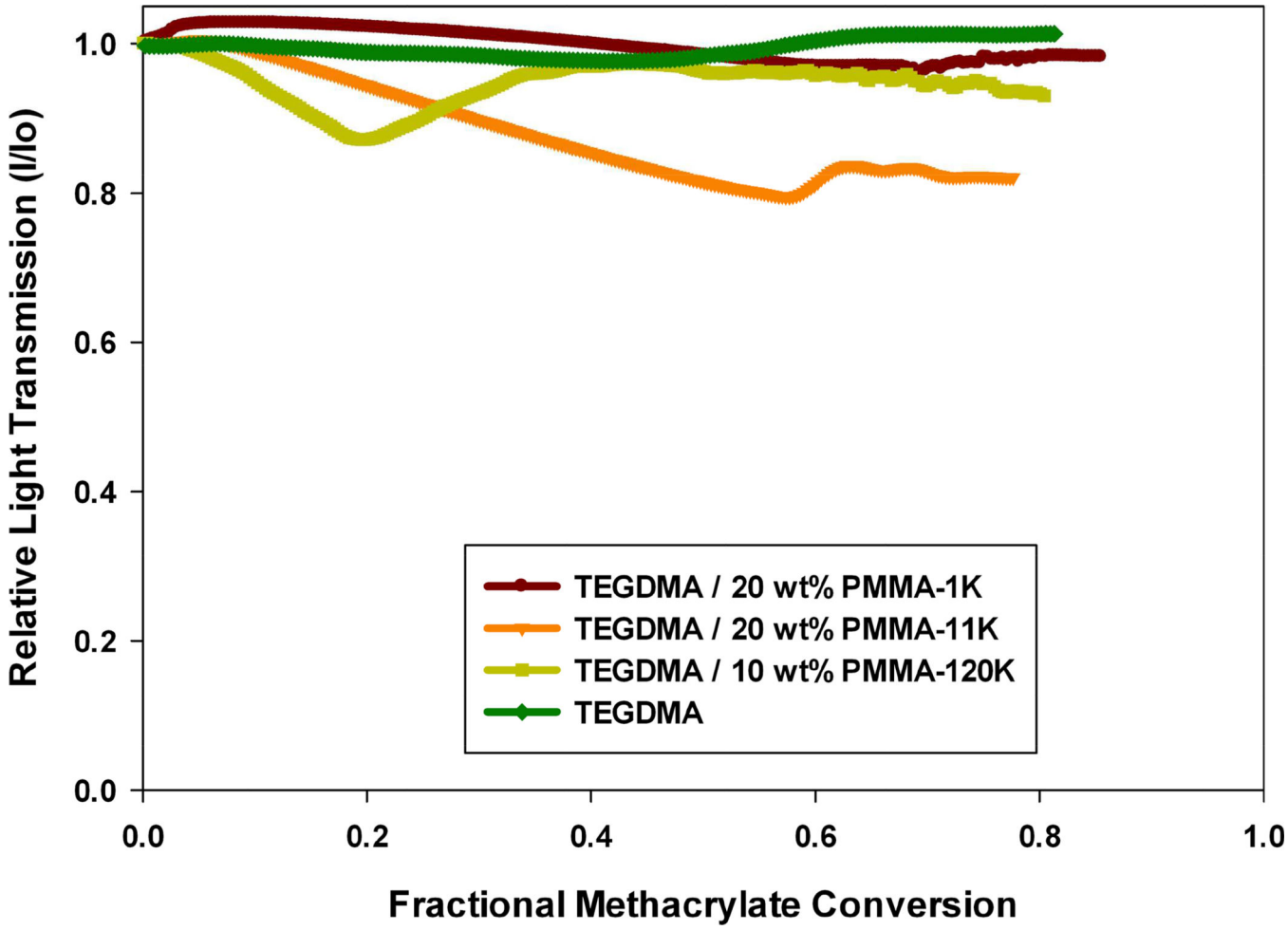

Figure 2.

Visible light transmission behavior during polymerization. Samples cured with UV-irradiation, I_o=5 mW/cm^2, λ=365 (±10 nm). Visible light transmission probed by monitoring λ=600 nm.

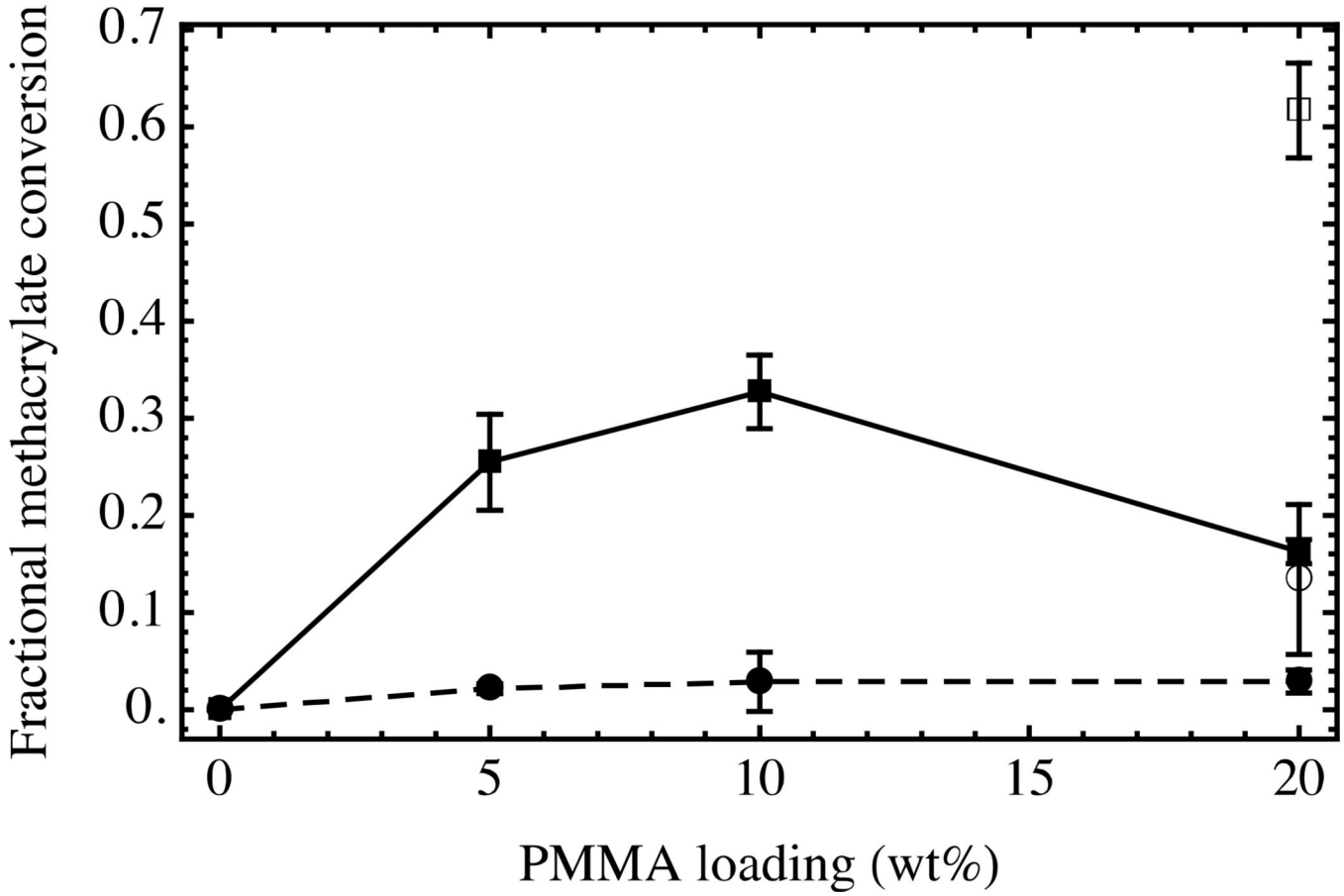

Figure 3.

Phase separation for TEGDMA matrices modified by PMMA-120K (shaded symbols) and PMMA-11K (open symbols). The onset of PIPS (circles) is taken as onset of turbidity in polymerizing resin, characterized by changes in visible light transmission (λ=600 nm). The minimum visible light transmission observed (squares) is used to indicate the end of phase separation during polymerization. Samples cured with UV-irradiation, I_o=5 mW/cm^2, λ=365 (±10 nm).

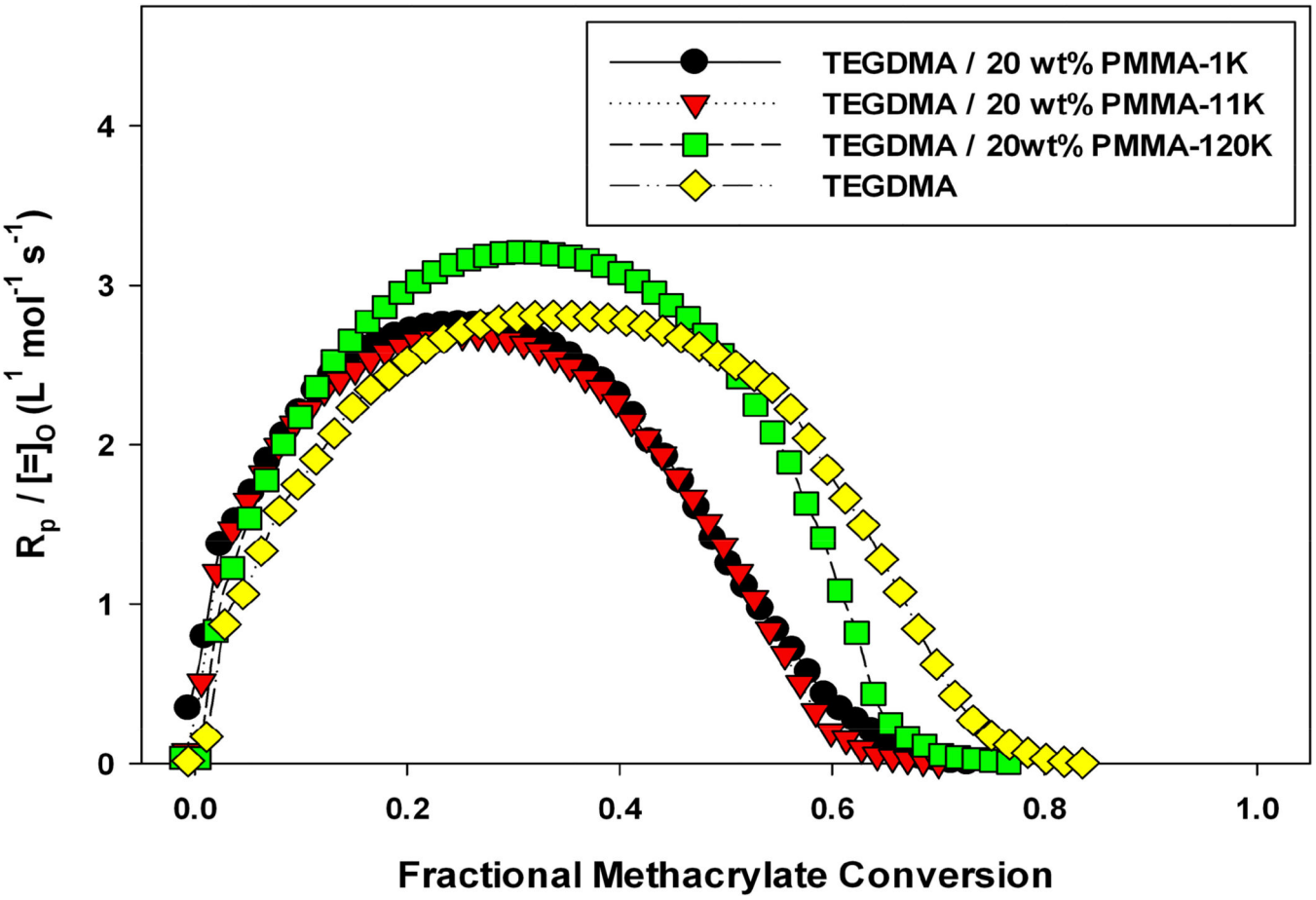

Figure 4.

Rate of polymerization rate (R_p), development in PMMA-modified matrices, I_o=300 μW/cm^2. All series are normalized by initial double bond concentration $[C=C]_o$ to eliminate rate concentration differences between prepolymer modified and un-modified systems.

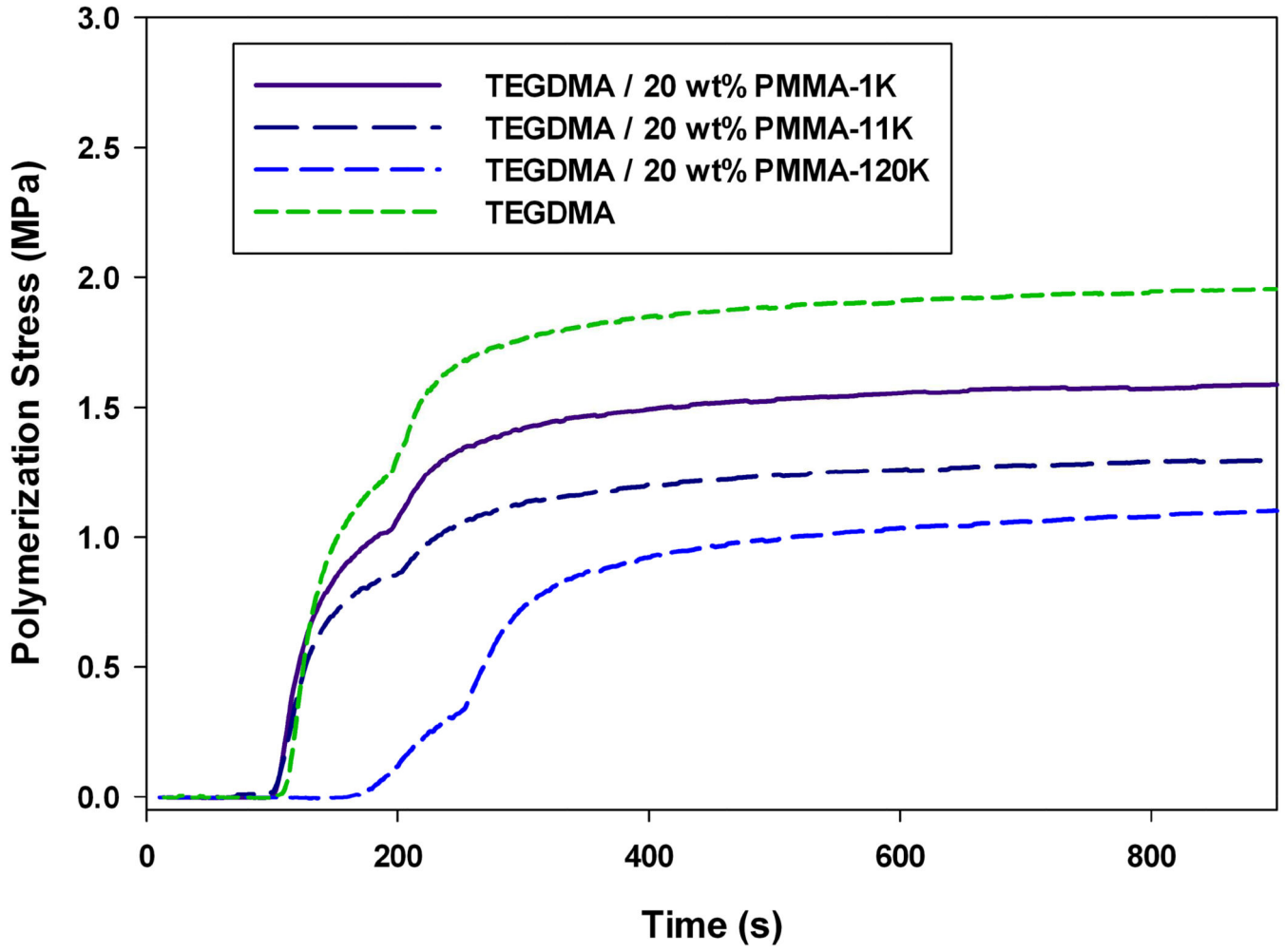

Figure 5.

Real-time polymerization stress of TEGDMA matrices modified by PMMA of varying molecular weights. Irradiation begins at 70 s, I_o= 300 μW/cm^2 until ~50% methacrylate conversion, and then I_o=20 mW/cm^2 for the remainder of the reaction.

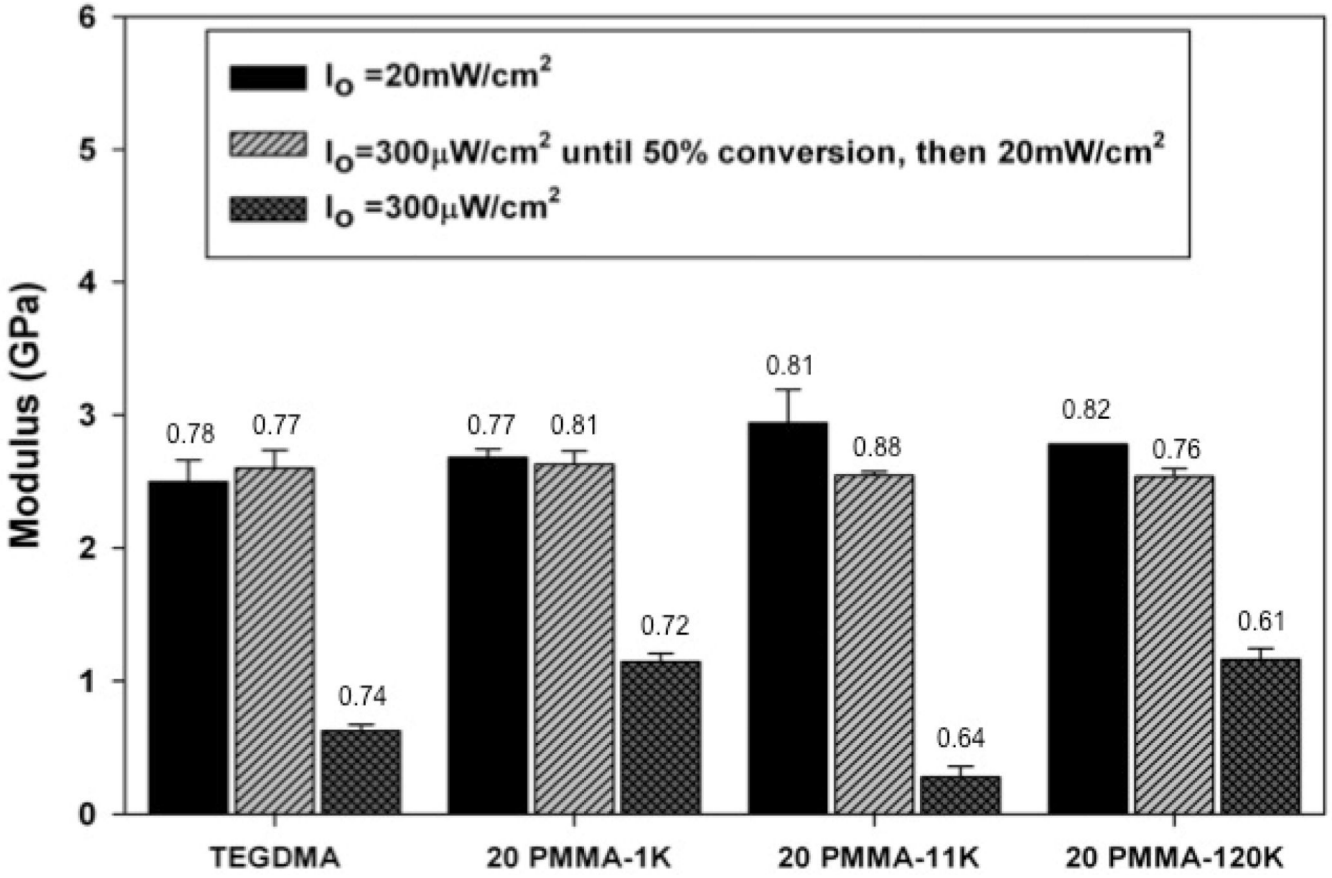

Figure 6.

Bulk elastic modulus of networks post-ambient photopolymerization at varying irradiation intensities and patterns. Average limiting fractional methacrylate conversion is denoted above each data set (n=3).

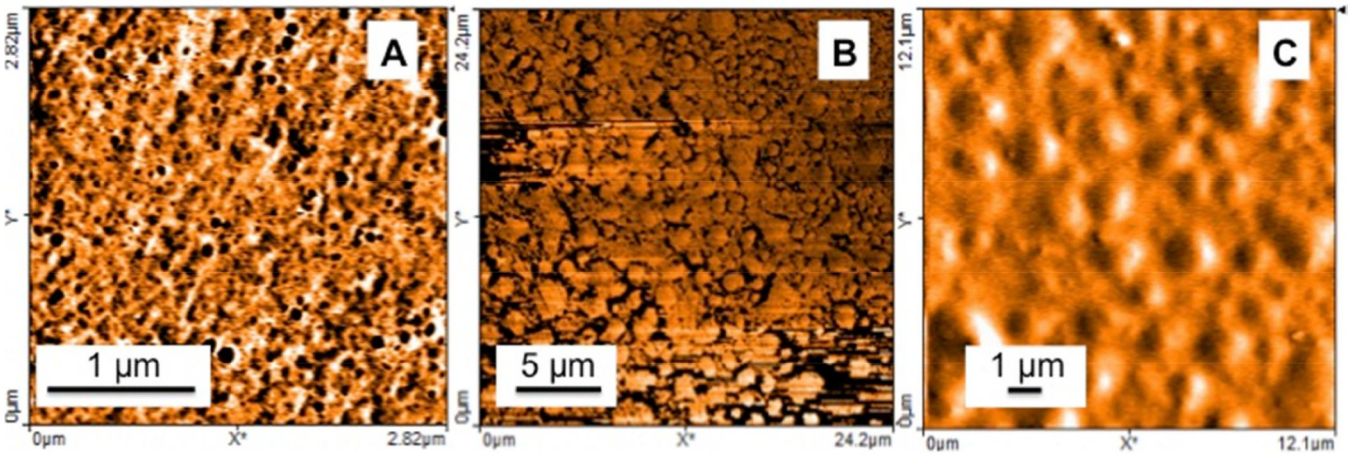

Figure 7.

AFM images, poly(TEGDMA) / 20 wt% PMMA-11K, post ambient photopolymerization. (A) I_o=20 mW/cm^2 (B) I_o=300 µW/cm^2 until ~50% methacrylate conversion, then I_o=20 mW/cm^2 for the remainder of the reaction (C) I_o=300 µW/cm^2 until ~50% methacrylate conversion, then I_o=20 mW/cm^2 or the remainder of the reaction.

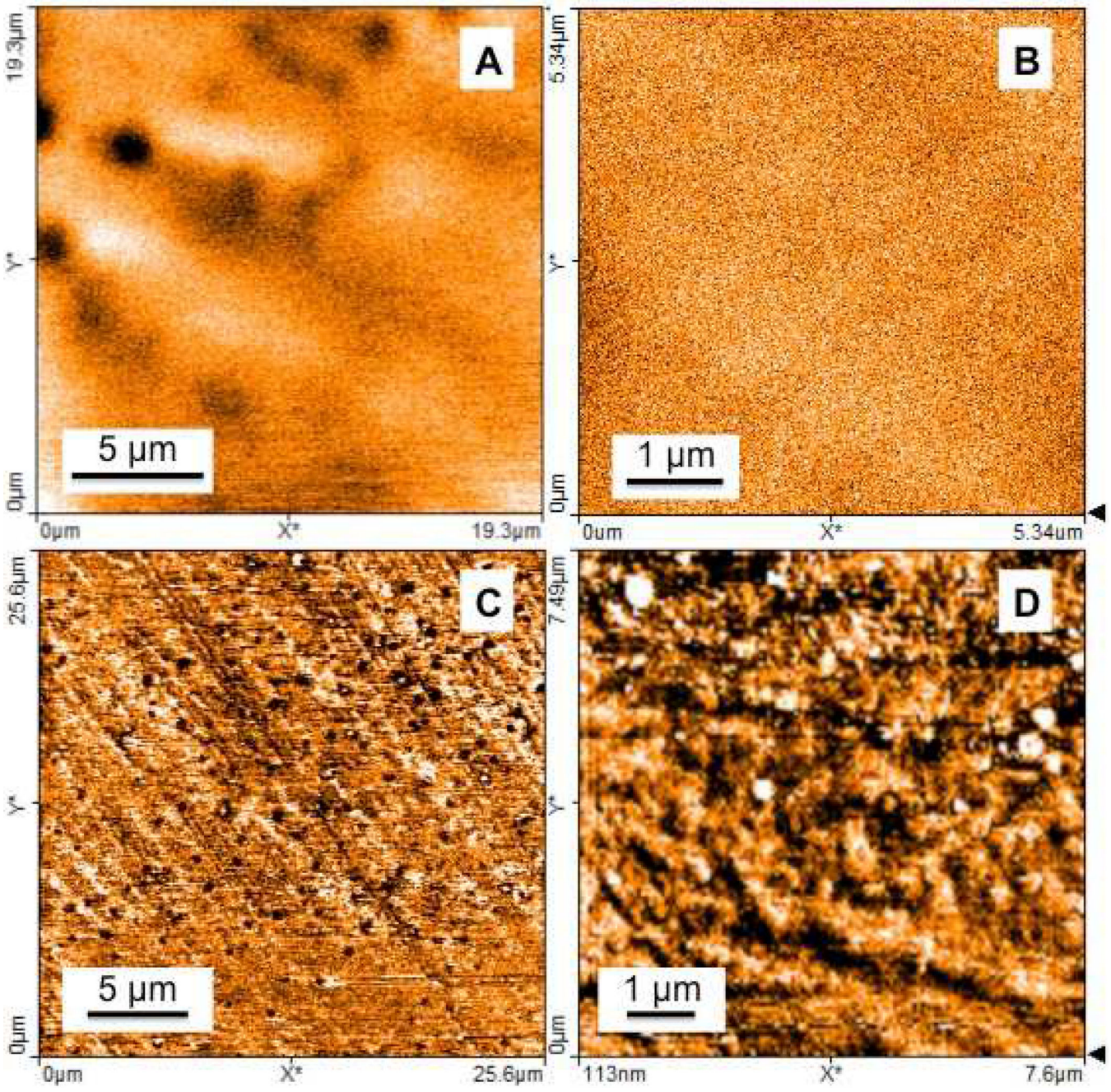

Figure 8.

AFM images, poly(TEGDMA) / 20 wt% PMMA-120K, post-ambient photopolymerization. (A) I_o=20 mW/cm^2 (B) I_o=20 mW/cm^2 (C) I_o=300 μW/cm^2 until ~50% methacrylate conversion, then I_o=20 mW/cm^2 for the remainder of the reaction (D) I_o=300 μW/cm^2 until ~50% methacrylate conversion, then I_o=20mW/cm^2 for the remainder of the reaction.

Table 1

Prepolymer Properties

PMMA (1kDa)	**PMMA (11kDa)**	**PMMA (120kDa)**
M_W~1,600 Da	M_W~11,700 Da	M_W~120,000 Da
PDI ~1.2	PDI ~1.5	PDI ~1.8
T_g~45 °C	T_g~74 °C	T_g~117 °C
$n_D^{25}=1.510(\pm 4\mathrm{E}{-4})$	$n_D^{25}=1.501(\pm 4\mathrm{E}{-4})$	$n_D^{25}=1.491(\pm 7\mathrm{E}{-4})$

Table 2

Average TEGDMA fraction in phase-separated materials (n=3)

	TEGDMA/ 20 wt% PMMA-11K	**TEGDMA/ 20 wt% PMMA-120K**
TEGDMA-rich	0.97 (± 1 E-1)	1.0 (± 2 E-1)
TEGDMA/ PMMA-rich	0.60 (± 4 E-2)	0.35 (± 4 E-2)

Table 3

Monomer/Prepolymer Solution Viscosities (n=3)

Sample	Viscosity (Pa*s) (E-02)
TEGDMA	1.09 (±0.05)
TEGDMA / 20 wt% PMMA-1K	1.79 (±0.17)
TEGDMA / 20 wt% PMMA-11K	5.75 (±1.2)
TEGDMA / 20 wt% PMMA-120K	283 (±6.0)